Transactions, SMiRT-25
Charlotte, NC, USA, August 4-9, 2019
Division IV

THE CAUSE OF DESTRUCTIVE GROUND MOTIONS ON THE BASIS OF STRONG MOTION RECORDS FROM JAPAN AND OTHER COUNTRIES

Daiki Imoto[1], Takashi Nakao[2], Tomoharu Mori[2], Koji Kakiuchi[3], Jiro Akashi[4], Kentaro Motoki[5], Kenichi Kato[6], Yusuke Tomozawa[7], and Yoshiyuki Takahashi[8]

[1]Kyushu Electric Power Co. INC., Fukuoka, Japan (Daiki_Imoto@kyuden.co.jp)
[2]Kyushu Electric Power Co. INC., Fukuoka, Japan
[3]Chief Manager, Kyushu Electric Power Co. INC., Fukuoka, Japan
[4]Deputy General Manager, Kyushu Electric Power Co. INC., Fukuoka, Japan
[5]Senior Manager, Kobori Research Complex INC., Tokyo, Japan
[6]Duputy Director, Kobori Research Complex INC., Tokyo, Japan
[7]Manager, Kobori Research Complex INC., Tokyo, Japan
[8]Kajima Corp., Tokyo, Japan

ABSTRACT

We collected observation records of damage caused by earthquakes that occurred both within and outside of Japan. We extracted records of seismic intensity 7 or 6 upper, and arranged the requirement conditions under which seismic intensity 7 might occur. We also examined the applicability of those conditions based on historical earthquakes and numerical analysis data. Finally, we reported the situations that would cause seismic intensity 7.

INTRODUCTION

For strong motion prediction and earthquake disaster prevention planning, it is important to indicate which cases will cause high-amplitude ground motions, such as seismic intensity 7 on the Japan Meteorological Agency (JMA) scale, which almost corresponds to seismic intensity X or greater on the modified Mercalli scale. Previous studies (Midorikawa and Goso, 1997, Takemura et al., 1998, and Miyazawa and Mori, 2006) noted that a large site amplification factor contributed to the occurrence of seismic intensity 7. This was in addition to a short distance from the seismic fault, from a quantitative point of view. Strong motion networks in Japan have been developed since the 1995 Kobe earthquake, and we can now qualitatively reconsider which parameters would cause seismic intensity 7.

In this paper, we made data sets with seismic intensity 7 and 6 upper obtained not only in Japan but also in other countries. We included the areas of seismic intensity 7 of historical earthquakes and of prediction scenario earthquakes calculated by the Japan Seismic Hazard Information Station (J-SHIS). Then, we extracted the differences between them in terms of closest distances, the average shear wave velocity to a depth of 30 m (AVS30), etc. Finally, we summarized the requirement conditions that caused seismic intensity 7.

DATA

We collected the strong motion records of seismic intensity 7 and 6 upper, the areas of seismic intensity 7 of historical earthquakes, and the distribution of seismic intensity 7 estimated by numerical calculation. We

searched for records of seismic intensity 7 in Japan from all publicly opened records and for those of seismic intensity 6 upper from the National Research Institute for Earth Science and Disaster Resilience (NIED) website, for earthquakes in Japan that occurred before 2016. For records outside of Japan, we collected 2620 acceleration records of 112 earthquakes that occurred from 1935 to 2016. Then, we evaluated the measured seismic intensity of all the records, and picked up the records of seismic intensity 7 and 6 upper. Figure 1 show the source mechanisms of the earthquakes for which the records of seismic intensity 7 and 6 upper were obtained. Seismic intensity 7 is caused by inland crustal earthquakes, except for the 2011 off the Pacific coast of Tohoku earthquake (hereafter, the 2011 Tohoku earthquake).

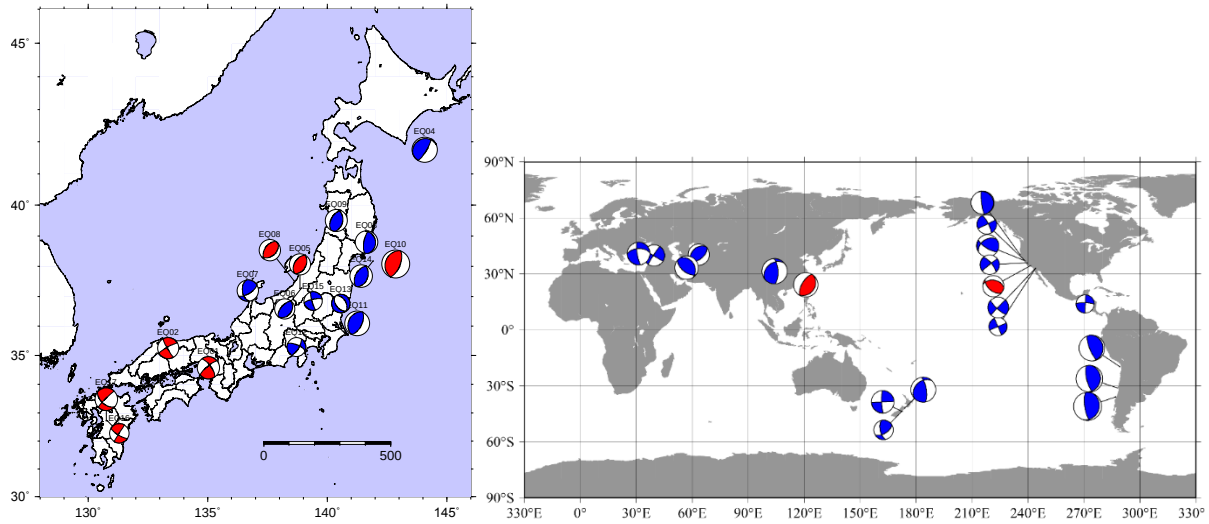

Figure 1. Focal spheres of the earthquakes in which the maximum seismic intensity was 7 (red) or 6 upeer (blue) occurring in Japan (left panel) and outside of Japan (right panel).

Among the historical earthquakes that occurred in recent decades, the 1995 Hyogoken–Nanbu earthquake (hereafter, the 1995 Kobe earthquake) and the 1948 Fukui earthquake were targeted. The area of seismic intensity 7 in the 1995 Kobe earthquake was published by the JMA (1997). Because seismic intensity 7 was not yet defined in 1948, we decided that the area of seismic intensity 7 would be based on the definition of seismic intensity 7 established in 1949: the area with a total collapse rate of wooden houses of 30% or more. The distribution of seismic intensity 7 for the 1995 Kobe earthquake and the 1948 Fukui earthquake is shown in Figure 2.

We also collected the numerical calculation results of scenario earthquakes for the Uemachi fault, Kego fault, and Tachikawa fault, which were located beneath urban areas. The numerical calculation results used in this study were evaluated by J-SHIS. Calculations were done for a total of 14 cases: six cases in the Uemachi fault, four cases in the Kego fault, and four cases in the Tachikawa fault. The different points in each case were the fault position, rupture start point, and strong motion generation area position. We used all of the calculations. The measured seismic intensity on the ground surface was calculated by adding an empirical amplification factor to the motions calculated on engineering bedrock using the stochastic Green's function method and the finite difference method. The surface seismic intensity is published with a 250-m mesh, and we extracted the mesh of seismic intensity 7. The numerical calculation data were used in the examination of the distance range, mentioned later.

The closest distance from the seismic fault (hereafter, closest distance), AVS30, and topographical classification were used to arrange the requirement conditions of seismic intensity 7. The AVS30 was obtained from the ratio of the 30-m thickness to the S-wave vertical travel time using a subsurface structure

model. The subsurface model was published up to at most a depth of 20 m at the K-NET stations. Therefore, we converted the AVS20 to AVS30 based on the empirical formula of Kanno et al. (2006). When the PS logging result was not obtained up to a depth of 20 m, it was assumed that the lowermost layer continued to that depth.

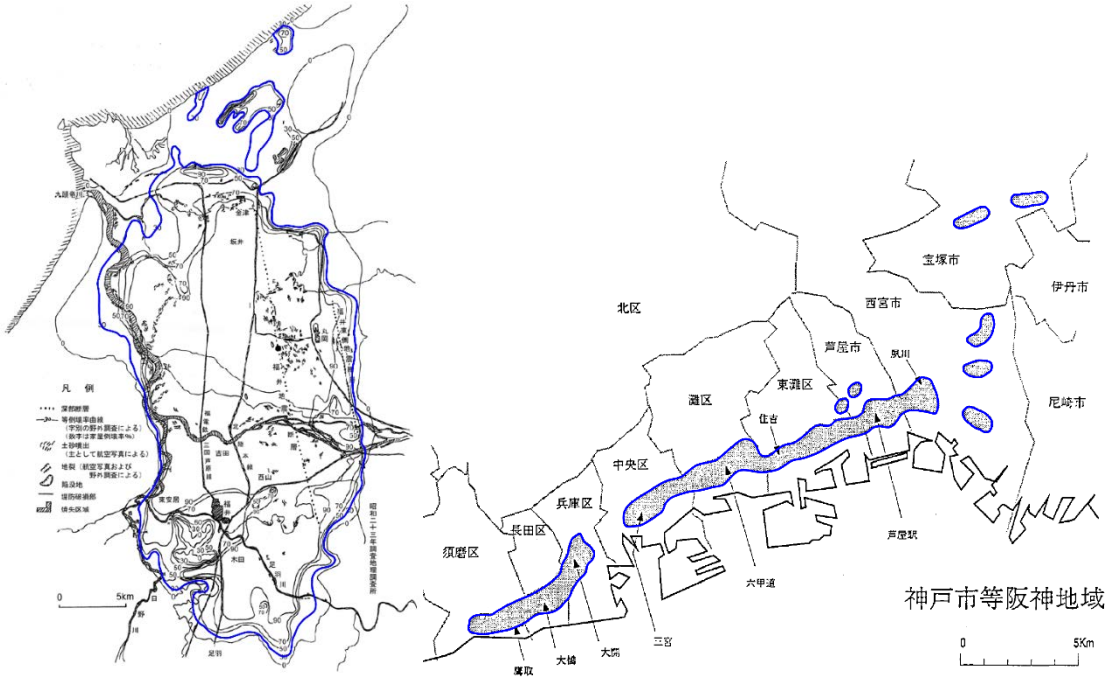

Figure 2. The area of seismic intensity 7 of the 1995 Hyogoken–Nanbu earthquake (right) and the 1948 Fukui earthquake (left). The grey shaded area enclosed by blue lines in the right figure shows the area of seismic intensity 7 published by the JMA. The area enclosed by blue lines in the left figure shows the area of seismic intensity 7 based on the total collapse rate of wooden houses.

We preferentially used subsurface models that had been published in previous studies based on microtremor array exploration, etc. For sites where there was no subsurface model, the AVS30s published by the J-SHIS were used in Japan and that published in the flat file of NGA-West 2 were used outside of Japan. The topographical classification was applied to data from within Japan, and the data published by the J-SHIS were referenced. The closest distance was evaluated using the fault model proposed by previous research. For earthquakes for which no fault model has been released, hypocentral distances were used. Most of the overseas records were referenced to the NGA-West 2 flat file.

A comparison of the pseudo velocity response spectra of the records of seismic intensity 7 and 6 upper is shown in left panel of Figure 3. Because the square root of sum of squares (SRSS) of the filtered waveforms of each component was used in calculating the measured seismic intensity, we adopted RotD100 proposed by Boore (2010), which is equivalent to the SRSS of the horizontal component. In a short-period range of about 0.5 seconds, the amplitudes of the records of seismic intensity 7 are not always higher than those of seismic intensity 6 upper. We can see that the peak values of seismic intensity 7 are higher than those of seismic intensity 6 upper and that the peak period of seismic intensity 7 tends to longer than those of seismic intensity 6 upper. The extracted predominant periods and peak values are shown in right panel of Figure 3. When obtaining the measured seismic intensity, a band pass filter with a period of 0.1 to 2.0 seconds is usually applied, so we focused on this period range. In addition, we distinguish inland earthquakes from subduction earthquakes. The peak values of the seismic intensity 7 records tend to be higher than those of upper records.

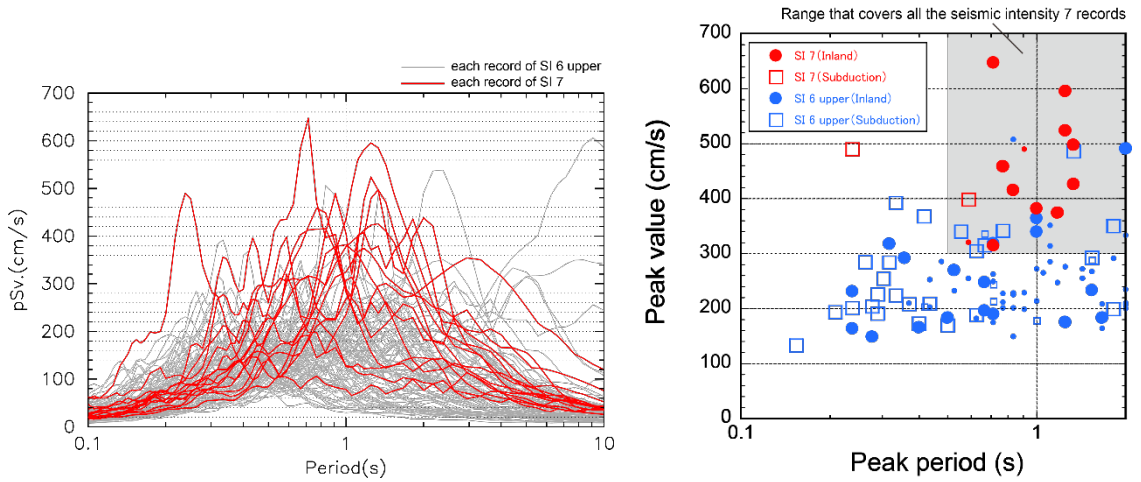

Figure 3. (Left panel) Comparison of pseudo velocity response spectra (RotD100, h = 0.05) for records of seismic intensity 7 (red lines) and 6 upper (grey lines). (right panel) Distributions of the predominant period and peak value of the pseudo velocity response spectra are shown in the left panel for the period range from 0.1 to 2 seconds. The large and small plots indicate data within and outside of Japan, respectively.

REQUIREMENT CONDITIONS FROM STATION DATA

We arranged the records of seismic intensity 7 and 6 upper from the point of view of the AVS30, topography, and closest distance. Figure 4 shows a comparison of the probability distribution of the AVS30s of the records of seismic intensity 7 and 6 upper. All the AVS30s of the seismic intensity 7 records are 350 cm/s or less; this distribution is biased to the lower side compared with that of seismic intensity 6 upper. The seismic intensity 7 records can be considered to have contributed to the amplification of the surface geology. Some seismic intensities of 6 upper occurred even with an AVS30 of 400 m/s or more, which is conventionally used as an engineering basement. Next, we arranged with the closest distance. The earthquakes that observed a seismic intensity 7 were inland earthquakes, except for the 2011 Tohoku earthquake; therefore, we focused on only such earthquakes when arranging the distances. A comparison of the distribution of the closest distances is shown in the right panel of Figure 4. In Japan, seismic intensity 7 occurs in a shorter distance range than seismic intensity 6 upper. As for the overseas records, we can see an opposite tendency to the Japanese records.

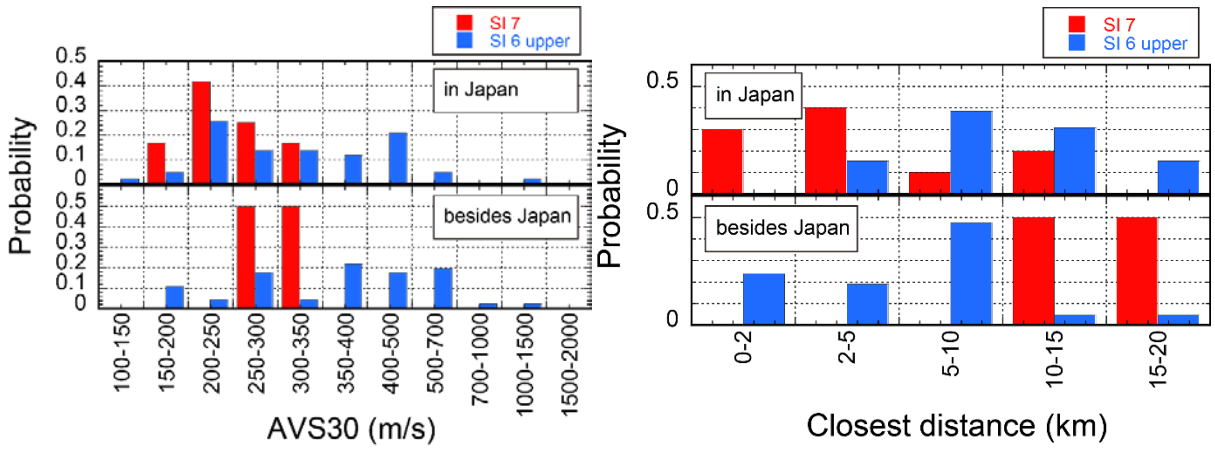

Figure 4. Probability distribution of the AVS30s and closest distances of stations at which seismic intensity of 7 and 6 upper were recorded.

The closest distance of two records with seismic intensity 7 occurred outside of Japan: 11.2 km for TCU 084 and 15.6 km for Tarzana. According to previous research, TCU084 and Tarzana are located at the tops of hills which may have topographic effects on earthquake motions. It has been confirmed from aftershock observations that Tarzana had topographical amplification effects (Spudich et al., 1996). In addition, the peak ground accelerations (PGAs) at stations less than 2 km away from Tarzana during the 1994 Northridge earthquake were about one seventh of that at Tarzana. In addition, during the 1987 Whittier Narrows earthquake, PGAs at Tarzana were significantly larger than those in other records for similar hypocentral distances from Tarzana (Shakal et al., 1988). The site amplification at Tarzana can be considered significantly large.

Finally, we arranged the topographical classifications. For the fine topography classification, only Japan was targeted because we could obtain data through the J-SHIS website. In order to understand trends in the distribution of topographical categories that are not continuous quantities, Figure 5 shows a comparison of the distribution of seismic intensity 7, not only with that of seismic intensity 6 upper but also with that of K-NET and KiK-net stations. There are several stations with seismic intensity 7 that are located on a classification that can be associated with a relatively stiff site, such as mountain foothill areas and plateaus. This is thought to be because the AVS30 is low, even in that category. Although there were no observation points classified as hills in the Japanese records, as mentioned above, TCU 084 and Tarzana are located on hills.

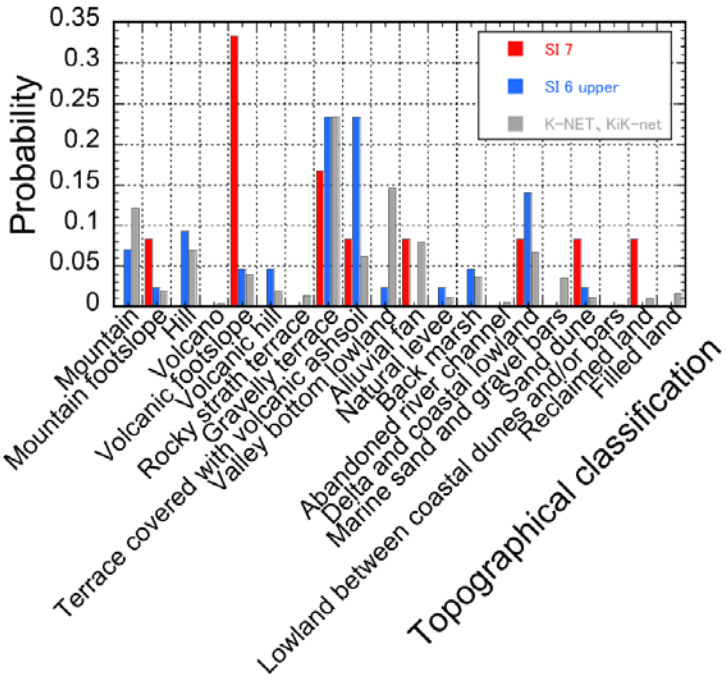

Figure 5. Probability distribution of the topographical classifications of stations at which seismic intensity of 7 and 6 upper were recorded.

We arranged the characteristics according to three factors. When the AVS30 was low, and the topography is foothills, a plateau, or a classification to be associated with soft surface geology, seismic intensity 7 might have occurred. According to Figure 4, the requirement of the AVS30 for seismic intensity 7 can be set as less than 350 m/s, but we set the threshold as 400 m/s, considering that the number of records was limited. In the topographical classification, in addition to the abovementioned mountainous areas and plateaus, divisions with softer surfaces such as triangles were added to the requirements for seismic intensity 7.

Summarizing the above examination, it is considered that seismic intensity 7 occurs when all of the following conditions are met when M ≧ 6.5： 1) the AVS30 is less than 400 m/s; 2) the topographical classification is not mountainous, volcanic, or rocky strath terrace; and 3) the closest distance is less than 15 km. As mentioned above, Tarzana slightly exceeds the third condition, even though the site amplification could be expected significantly larger than at other stations. Tarzana can be considered to almost meet the above three conditions.

REQUIREMENT FROM HISTORICAL AND PREDICTION DATA

In order to confirm the applicability of the required conditions of seismic intensity 7 obtained from observation records, we examined whether the distribution of seismic intensity 7 due to historical earthquakes could be predicted. The fault models of the 1948 Fukui earthquake and the 1995 Kobe earthquake are referred to by Ichinose et al. (2005) and Cho and Nakanishi (2000), respectively. The AVS30s and topographical classification are referred to by the J-SHIS. Figure 6 shows a comparison of the actual area of seismic intensity 7 and the predicted area that meets all of the requirement conditions mentioned above.

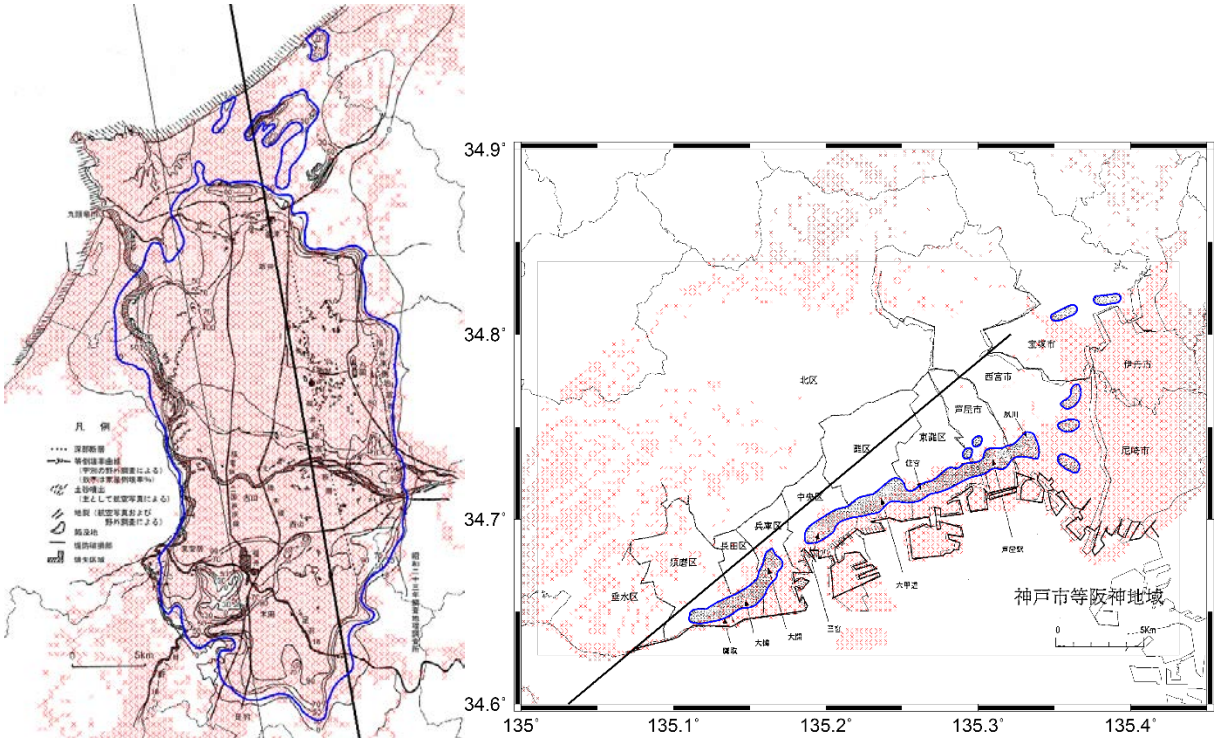

Figure 6. Comparison of the areas (shown with red crosses) that meet the requirement conditions for seismic intensity 7 with the actual areas of seismic intensity 7 (enclosed by blue lines), which were based on the total collapse rate of wooden houses.

In the 1948 Fukui earthquake, shown in the left panel, the predicted area corresponds well to the area of seismic intensity 7. In the 1995 Kobe earthquake, shown in the right panel, most of the areas in the so-called damage belt could be predicted. We had some areas that could not be predicted, e.g., in Nada ward and part of Ashiya City. Moreover, the predicted area was widely spread, even in the areas that were not seismic intensity 7.

In order to show how the range of seismic intensity 7 could be predicted from wooden house damage, the coverage rate was evaluated. The coverage rate is expressed by the ratio of the areas successfully predicted by this study to the areas of seismic intensity 7. For the 1948 Fukui earthquake, the coverage rate was 97.4% and for the 1995 Kobe earthquake it was 72.9%. For the Kobe earthquake, we targeted only the Kobe area, including Ashiya, Nishinomiya, and Takarazuka but excluding the island of Awaji. Although the seismic intensity 7 of the Fukui earthquake was almost predictable, that of the 1995 Kobe earthquake was predicted to be only about 70%.

We surveyed the effective factors that contributed to the failed result. Figure 7 shows the rates that did not meet the conditions of each factor. The rate for the AVS30 was 100%, and that for the closest distance was 0% for both earthquakes. That is, the main reason why seismic intensity 7 could not be predicted is that the threshold of the AVS30 was low. Then, the distribution of the AVS30 in the area where seismic intensity 7 could not be predicted was surveyed, as shown in Figure 8. Most of the AVS30s were less than 500 m/s. When the threshold was raised to 500 m/s, the abovementioned coverage rate changed from 97.8% to 99.6% in the Fukui earthquake; in the Kobe earthquake, it improved from 72.9% to 99.1%. Because the purpose of this study was to present the requirement conditions for the coverage to be close to 100%, the threshold of the AVS30 was changed from 400 to 500 m/s.

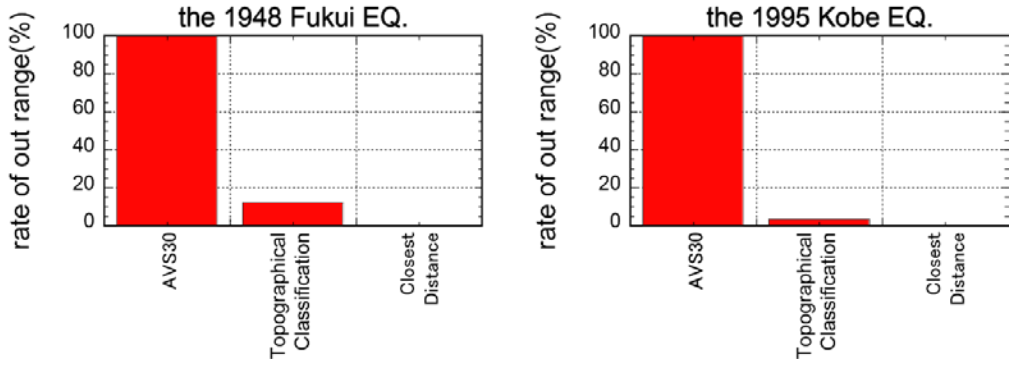

Figure 7. Rates of each factor that did not evaluate the actual seismic intensity 7 with the requirement conditions.

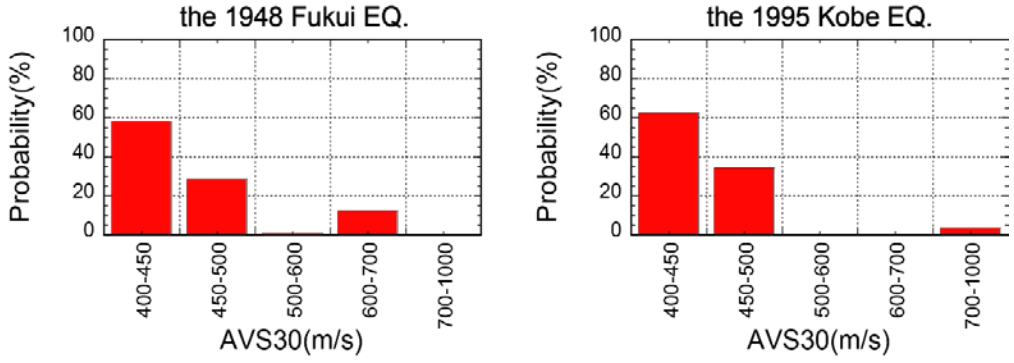

Figure 8. Probability distribution of AVS30s over 400 m/s in the area of seismic intensity 7.

Looking at the application to the 1995 Kobe earthquake shown in right panel of Figure 6, the requirement conditions predicted a much wider area than the actual area of seismic intensity 7. Although our aim was to establish the requirement conditions, it was desirable to suppress overestimation as much as possible; therefore, we investigated the valid distance threshold based on the area of seismic intensity 7 of historical earthquakes and numerical analysis results. The probability distribution for the closest distance

of seismic intensity 7 was evaluated, and the distance at which the significance level was 5% was determined.

The distribution of seismic intensity 7 is more frequent in the short distance range than that in the long distance range. Therefore, we adopted a gamma distribution function for fitting to the distribution of seismic intensity 7 in the closest distance. From the modeled distribution function, a distance exceeding the 5% significance level that is generally used for engineering purposes was determined. The distance at which the cumulative distribution function is 95% was also determined. Taking the Fukui earthquake of 1948 as an example, this is shown in Figure 9. The parameters k and ν of the gamma distribution were determined by a grid search so that the model function fit the red curve of the left panel, which represents the distribution of seismic intensity 7. From the cumulative distribution function and using these parameters, the distance at the significance level of 5% indicated by the arrow) was estimated. In this way, we calculated the distances of the significance level of 5% for two historical earthquakes and 14 numerical calculation results.

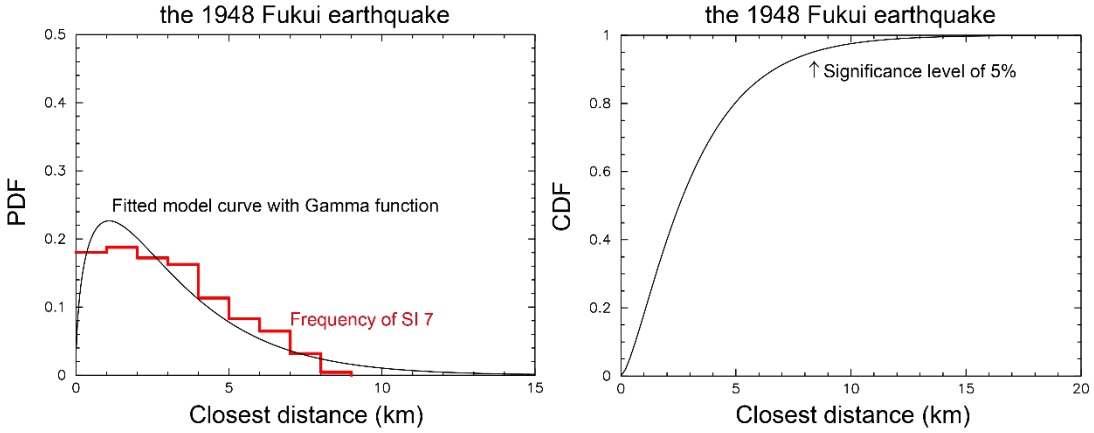

Figure 9. Gamma distribution (black line) approximated to the probability distribution (red line) of seismic intensity 7 with the closest distance shown in left panel and the cumulative distribution function of seismic intensity 7 with the closest distance and distance of significance level of 5% shown in right panel.

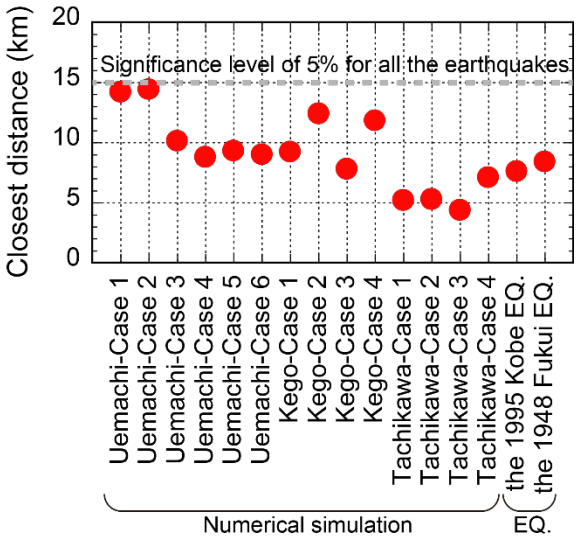

Figure 10. Distance of significance level of 5% of seismic intensity 7 when assuming a gamma distribution.

The results are shown in Figure 10. The distance is less than 10 km for most earthquakes but more than 10 km for the Uemachi and Kego faults. In order to cover all earthquakes, it was shown that it is appropriate to set the closest distance to 15 km. This distance was the same as that obtained from the strong motion records mentioned above. We proposed that the closest distance be less than 15 km as the requirement condition of seismic intensity 7.

DISCUSSION

The requirement conditions shown here are those that must be set to avoid missing seismic intensity 7; there can be many predicted points where that intensity will not occur. We applied these conditions to the records of inland earthquakes in Japan. The results are shown in Table 1. Ten of the 18 records of seismic intensity 6 upper met the requirement conditions. The predicted seismic intensity 7 in this study tends to overestimate rather than accurately predict the seismic intensity. This condition is considered as an indicator that presents the possibility of occurrence of high-amplitude earthquake motions of seismic intensity 7 for important structures that have to resist earthquake motions. As an example, Table 1 shows the results applied to Kyushu Electric Power's Genkai and Sendai sites. Faults of scenario earthquakes at both sites were set at the position where the closest distance was less than 15 km, but it was confirmed that the AVS30 was more than 1000 m/s at both sites and the topographical classification did not satisfy the conditions. Therefore, even if an inland earthquake occurs in the vicinity of the Genkai and Sendai sites, the possibility of occurrence of seismic intensity 7 is considered to be low.

Table 1: Classification of the AVS30, topographical classification, and closest distance of the sites where intensity 6 strong records were observed during an inland earthquake in Japan

earthquake	site	AVS30			T. C.		C. D.		M_J	All factors	
		①	②	③	④	⑤	⑥	⑦			
the 1995 Kobe earthquake	Takatori	●			●		●		7.3	●	SI 7
the 1995 Kobe earthquake	Fukuiai	●			●		●		7.3	●	
the 2000 Tottoriken-seibu earthquake	TTRH02	●			●		●		7.3	●	
the 2004 Niigataken Chuetsu earthquake	NIG019	●			●		●		6.8	●	
the 2004 Niigataken Chuetsu earthquake	Kawaguchi	●			●		●		6.8	●	
the 2007 Niigataken Chuetsuoki earthquake	KK site	●			●		●		6.8	●	
the 2016 Kumamoto earthquake (M6.5)	Mashikimachi	●			●		●		6.5	●	
the 2016 Kumamoto earthquake (M7.3)	Nishiharamura	●			●		●		7.3	●	
the 2016 Kumamoto earthquake (M7.3)	Mashikimachi	●			●		●		7.3	●	
the 2016 Kumamoto earthquake (M7.3)	KMMH16	●			●		●		7.3	●	
the 2016 Kumamoto earthquake (M6.5)	KMMH16	●			●		●		6.5	●	SI 6 upper
the 2008 Iwate-Miyagi nairiku earthquake	AKTH04	●			●			●	7.2		
the 2008 Iwate-Miyagi nairiku earthquake	IWTH25		●		●		●		7.2		
the 2011 Fujinomiya earthquake	SZO011	●			●			●	6.4		
the 2007 Niigataken Chuetsuoki earthquake	NIG018	●			●		●		6.8	●	
the 2007 Noto hanto earthquake	ISK005	●			●		●		6.9	●	
the 2016 Kumamoto earthquake (M7.3)	KMM008	●			●		●		7.3	●	
the 2004 Niigataken Chuetsu earthquake	NIG021	●			●		●		6.8	●	
an aftershock of the 2004 Niigataken Chuetsu earthquake	NIG021	●			●		●		6.5	●	
the 2016 Kumamoto earthquake (M7.3)	KMMH03	●			●			●	7.3		
the 2004 Niigataken Chuetsu earthquake	NIGH01	●			●		●		6.8	●	
the 2004 Niigataken Chuetsu earthquake	NIG028	●			●		●		6.8	●	
the 2016 Kumamoto earthquake (M7.3)	KMM006	●			●		●		7.3	●	
the 2016 Kumamoto earthquake (M7.3)	OIT009	●			●			●	7.3		
the 2008 Iwate-Miyagi nairiku earthquake	IWTH26	●			●		●		7.2	●	
an aftershock of the 2004 Niigataken Chuetsu earthquake	NIG019	●			●			●	6.5		
the 2011 northern Ibaraki earthquake	IBRH13	●				●	●		6.1		
the 2013 northern Tochigi earthquake	TCGH07	●				●	●		6.3		
Scenario earthquakes	Genkai site			●		●	●		6.9-7		
Scenario earthquakes	Sendai site			●		●	●		7.2-7.6		

T. C. : Topographical Classification, C. D. : Closest Distance
AVS30 : ①AVS30<400、②400≦AVS30<1000、③AVS30≧1000
T. C. : ④except Mountain, Volcano, nor Rocky strath terrace, ⑤ Mountain, Volcano, or Rocky strath terrace
C. D. : ⑥C. D. <15km、⑦C. D.≧15km

CONCLUSION

The strong motion records for earthquakes within and outside of Japan were collected, the distribution of seismic intensity 7 obtained based on the wooden house damage rate of historical earthquakes was investigated, and the strong motion prediction results by active faults located under the city were organized. The concluding remarks are the following.

1. Seismic intensity 7 occurred in inland earthquakes of M6.5 or more, with the exception of the 2011 Tohoku earthquake. The features associated with seismic intensity 7 are that the predominant period of pSv is 0.5 seconds or longer and the peak value is 300 cm/s or higher.

2. Based on the three kinds of data for seismic intensity 7, the requirement conditions that may occur with seismic intensity 7 were categorized. A seismic intensity of 7 may occur when all three of the following conditions are met:

    1) AVS30 is less than 400 m/s
    2) Topographical classification is not mountainous, volcanic, or rocky strath terrace
    3) Closest distance is less than 15 km

3. When the conditions of the Genkai and Sendai sites were examined, the AVS30s and topographical classifications did not meet the requirement conditions and it was considered that the possibility of occurrence of seismic intensity 7 was low, even for an earthquake in the vicinity of each site.

REFERENCES

Boore, D. M. (2000). "Orientation-Independent, Nongeometric-Mean Measures of Seismic Intenxity from Two Horizontal Components of Motion," *Bull. Seism. Soc. Am.*, Vol. 100, 1830-1835.

Cho, I., and I. Nakanishi. (2000). "Investigation of the Three-Dimensional Fault Geometry Ruptured by the 1995 Hyogo-Ken Nanbu Earthquake using Strong-Motion and Geodetic Data," *Bull. Seis. Soc. Am.*, Vol. 90, 450-467.

Ichinose, G. A., P. Somerville, H. K. Thio, S Matsushima and T. Sato (2005). "Rupture process of the 1948 Fukui earthquake (M 7.1) from the Joint Inversion of Seismic Waveform and Geodetic Data," *J. Geophys. Res.*, 110 (B5) B05301, doi:10.1029/2004JB003437.

Japan Meteorological Agency. (1997). "Field survey, Report on the Hyogo-ken-nanbu Earthquake, 1995," *Technical Report of the Japan Meteorological Agency*, No. 119, 47-90.

J-SHIS: Japan Seismic Hazard Information Station, http://www.j-shis.bosai.go.jp/en/

Kanno T., A. Narita, N. Morikawa, H. Fujiwara and Y. Fukushima (2006). "A New Attenuation Relation for Strong Ground Motion in Japan Based on Recorded Data," *Bull. Seism. Soc. Am.*, 96, 879 -897.

Midorikawa, S. and Goso, T. (1997). "A Study on Occurrence Rate of Destructive Ground Motion Based on Case Histories," *J. Struct. Constr. Eng.*, AIJ, No. 502, 55-60. (in Japanese)

Miyazawa, M. and Mori, J. (2006). "Recorded Maximum Seismic Intensity Maps in Japan from 1586 to 2004," *Seism. Res. Lett.*, Vol. 77, 154-158.

Shakal, A., Huang, M. J., and Cao, T. Q. (1988), "The Whittier Narrows, California Earthquake of October 1, 1987-CSMIP Strong Motion Data," *Earthquake Spectra*, 4, 75-100.

Spudich, Paul, Hellweg, Margaret, and W. H. K. Lee (1996), "Directional Topographic Site Response at Tarzana Observed in Aftershocks of the 1994 Northridge, California, Earthquake: Implications for Mainshock Motions," *Bull. Seism. Soc. Am.*, Vol. 86, No. 1B, S193-S208.

Takemura, M., Moroi, T. and Yashiro, K. (1998). "Characteristics of Strong Ground Motions as Deduced from Spatial Distributions of Damages due to the Destructive Inland Earthquakes from 1891 to 1995 in Japan," *Zisin*, Vol. 50, 485-505. (in Japanese).